

# Downregulation of adenosine and adenosine A1 receptor contributes to neuropathic pain in resiniferatoxin neuropathy

Hung-Wei Kan<sup>a</sup>, Chin-Hong Chang<sup>b</sup>, Chih-Lung Lin<sup>c,d</sup>, Yi-Chen Lee<sup>e,f</sup>, Sung-Tsang Hsieh<sup>a,g,h</sup>, Yu-Lin Hsieh<sup>e,f,\*</sup>

## Abstract

The neurochemical effects of adenosine signaling in small-fiber neuropathy leading to neuropathic pain are yet to be explored in a direct manner. This study examined this system at the level of ligand (through the ectonucleotidase activity of prostatic acid phosphatase [PAP]) and adenosine A1 receptors (A1Rs) in resiniferatoxin (RTX) neuropathy, a peripheral neurodegenerative disorder that specifically affects nociceptive nerves expressing transient receptor potential vanilloid type 1 (TRPV1). We conducted immunohistochemistry on dorsal root ganglion (DRG) neurons, high-performance liquid chromatography for functional assays, and pharmacological interventions to alter PAP and A1Rs in mice with RTX neuropathy. In DRG of RTX neuropathy, PAP(+) neurons were reduced compared with vehicle-treated mice ( $P = 0.002$ ). Functionally, PAP ectonucleotidase activity was consequently reduced (ie, the content of adenosine in DRG,  $P = 0.012$ ). PAP(+) neuronal density was correlated with the degree of mechanical allodynia, which was reversed by intrathecal (i.t.) lumbar puncture injection of recombinant PAP with a dose-dependent effect. Furthermore, A1Rs were downregulated ( $P = 0.002$ ), and this downregulation was colocalized with the TRPV1 receptor ( $31.0\% \pm 2.8\%$ ). Mechanical allodynia was attenuated in a dose-dependent response by i.t. injection of the A1R ligand, adenosine; however, no analgesia was evident when an exogenous adenosine was blocked by A1R antagonist. This study demonstrated dual mechanisms of neuropathic pain in TRPV1-induced neuropathy, involving a reduced adenosine system at both the ligand (adenosine) and receptor (A1Rs) levels.

**Keywords:** Small-fiber neuropathy, Transient receptor potential vanilloid subtype 1, Prostatic acid phosphatase, Adenosine, Adenosine A1 receptor, Resiniferatoxin

## 1. Introduction

Adenosine signaling contributes to analgesia through its pleiotropic effects. Key components of this signaling pathway are (1) adenosine, which is a ligand for multiple adenosine receptors,<sup>1,9,23</sup> and (2) the transmembrane isoform of prostatic acid phosphatase (PAP), which hydrolyzes extracellular adenosine monophosphate

(AMP) into adenosine using its ectonucleotidase properties.<sup>35,37,47</sup> Prostatic acid phosphatase is widely expressed by nonpeptidergic small-diameter nociceptors<sup>40,41</sup> and nerve growth factor (NGF)-dependent peptidergic nociceptors,<sup>41</sup> implying that PAP plays a key role in the maintenance of the delicate balance between nociception and analgesia. Inflammatory pain was alleviated by intrathecal (i.t.) injection of recombinant PAP,<sup>35</sup> and nerve injury-induced neuropathic pain was enhanced in PAP-knockout mice.<sup>34,36,47</sup> These observations raised the critical questions, such as (1) how PAP is modulated after specific injury to small-diameter sensory nerves because most neuropathic pain models affect both large- and small-diameter sensory nerves, and (2) whether the dysregulation of adenosine system contributes to degeneration-induced neuropathic pain? Different adenosine receptors contribute to the analgesic effect of adenosine signaling,<sup>1,27,32,46</sup> in particular, functional adenosine A1 receptors (A1Rs),<sup>15,32,35,47</sup> and animals that lacking A1Rs exhibited increased nociceptive responses.<sup>16,42</sup> Acupuncture induces analgesia through an increase in purine nucleotides, particularly by increasing adenosine<sup>39</sup> and A1R activation.<sup>9,15</sup> These observations suggest that both adenosine and functional activations of A1Rs are essential for analgesia. However, the mechanism by which A1Rs are modulated after nerve injury remains unknown. Collectively, it remains unclear how this adenosine system is regulated at the level of ligand (determined by PAP ectonucleotidase activity) and receptor (A1R functional efficacy) to modulate neuropathic pain in systemic neuropathy specifically affecting nociceptive neurons.

Neuropathic pain is one of the key symptoms of human peripheral nerve disorders when small-diameter nociceptive nerves are affected. Many diseases such as diabetes mellitus

Sponsorships or competing interests that may be relevant to content are disclosed at the end of this article.

H.-W. Kan and C.-H. Chang contributed to this work equally.

<sup>a</sup> Department of Anatomy and Cell Biology, College of Medicine, National Taiwan University, Taipei, Taiwan, <sup>b</sup> Department of Surgery, Chi Mei Medical Center, Tainan, Taiwan, <sup>c</sup> Department of Neurosurgery, Kaohsiung Medical University Hospital, Kaohsiung, Taiwan, <sup>d</sup> Faculty of Medicine, Graduate Institute of Medicine, College of Medicine, Kaohsiung Medical University, Kaohsiung, Taiwan, <sup>e</sup> Department of Anatomy, School of Medicine, College of Medicine, Kaohsiung Medical University, Kaohsiung, Taiwan, <sup>f</sup> Department of Medical Research, Kaohsiung Medical University Hospital, Kaohsiung, Taiwan, <sup>g</sup> Department of Neurology, National Taiwan University Hospital, Taipei, Taiwan, <sup>h</sup> Graduate Institute of Brain and Mind Science, College of Medicine, National Taiwan University, Taipei, Taiwan

\*Corresponding author. Address: Department of Anatomy, College of Medicine, Kaohsiung Medical University, 100 Shih-Chuan 1st Rd, Kaohsiung 80708, Taiwan. Tel.: (886)-7-3121101; fax: (886)-7-3119849. E-mail address: yhsieh@kmu.edu.tw (Y.-L. Hsieh).

PAIN 159 (2018) 1580–1591

Copyright © 2018 The Author(s). Published by Wolters Kluwer Health, Inc. on behalf of the International Association for the Study of Pain. This is an open-access article distributed under the terms of the Creative Commons Attribution-Non Commercial-No Derivatives License 4.0 (CCBY-NC-ND), where it is permissible to download and share the work provided it is properly cited. The work cannot be changed in any way or used commercially without permission from the journal.

<http://dx.doi.org/10.1097/j.pain.0000000000001246>

and medical treatments such as chemotherapy cause degeneration of small-diameter nerves, resulting in neuropathic pain. However, these diseases frequently also involve larger-diameter sensory nerves, which makes exploring the specific roles of small fibers in neuropathic pain difficult. To eliminate the concern that large-fiber degeneration might cause neuropathic pain, we developed a mouse model of pure small-fiber neuropathy, in which small-diameter sensory nerves are specifically depleted by resiniferatoxin (RTX), a capsaicin analogue that acts on transient receptor potential vanilloid type 1 (TRPV1) receptors.<sup>12–14,18,24</sup> Previous studies have indicated that pronociceptive mechanisms in RTX neuropathy include an increase in purinocceptor P2X3<sup>12</sup> expression and a burst of ATP release due to degeneration of small-diameter nociceptors.<sup>12,18</sup> It is not clear whether the cellular analgesia system (ie, adenosine signaling) is altered in RTX neuropathy and contributes to neuropathic pain in addition to enhancement of the purinergic nociceptive system.

To address the aforementioned issues, this study aimed to determine (1) whether the ligand and receptor of adenosine signaling are altered in RTX neuropathy and (2) whether the change in adenosine signaling contributes to pain hypersensitivity in RTX neuropathy. Specifically, we examined PAP expression, adenosine content, and A1R expression in RTX neuropathy.

## 2. Material and methods

### 2.1. Induction of resiniferatoxin neuropathy

Resiniferatoxin neuropathy was induced by administering a single dose of an RTX (50 µg/kg; Sigma, St. Louis, MO) solution by using our previously established protocol.<sup>12,13,18,41</sup> Briefly, RTX was dissolved in a vehicle (10% Tween 80 and 10% ethanol in normal saline), and mice received the RTX solution through an intraperitoneal (i.p.) injection (RTX group). One group of mice received an equal volume of the vehicle as the control (vehicle group). After treatment, the mice were housed in plastic cages on a 12-hour light/12-hour dark cycle and were given access to water and food ad libitum. All procedures were conducted in accordance with the ethical guidelines for laboratory animals,<sup>44</sup> and the protocol was approved by Kaohsiung Medical University. All experimental procedures were performed carefully, and all efforts were made to minimize suffering.

### 2.2. Evaluation of mechanical allodynia

The mechanical threshold after RTX neuropathy developed was assessed using the up-and-down method with different calibers of von Frey monofilaments (Somedic Sales AB, Hörby, Sweden).<sup>12,18</sup> Briefly, a series of monofilaments were applied to the plantar region of the hind paw. If the paw was withdrawn, a monofilament of a smaller caliber was applied. In the absence of paw withdrawal, a monofilament of a larger caliber was then used. Four additional stimuli with monofilaments of different calibers as determined by previous responses were applied, and the mechanical threshold was calculated according to a published formula.<sup>4</sup>

### 2.3. Primary antisera

All primary antisera in this study were purchased from commercial laboratories, and the following antisera were used: anti-PAP (chicken, 1:600; Aves Labs, Tigard, OR), anti-TRPV1 (goat, 1:100; Santa Cruz Biotechnology, Santa Cruz, CA), anti-AMP-activated protein kinase (AMPK, rabbit, 1:200; Cell Signaling

Technology, Danvers, MA), and anti-A1R (rabbit, 1:300; Acris Antibodies GmbH, Herford, Germany) antisera.

### 2.4. Immunofluorescence staining of dorsal root ganglion neurons

We conducted double-labeling immunofluorescence staining to investigate the molecular complex of adenosine signaling. The mice were killed through intracardiac perfusion with 0.1 M phosphate buffer (PB) followed by 4% paraformaldehyde (4P) in 0.1 M PB. The fourth and fifth (L4/L5) lumbar dorsal root ganglion (DRG) tissues were removed carefully after perfusion and fixed in 4P for another 6 hours. Dorsal root ganglion tissues were cryoprotected with 30% sucrose in 0.1 M PB overnight and cryosectioned with a cryostat (CM1850; Leica, Wetzlar, Germany) at an 8-µm thickness. For adequate sampling, 2 ganglia (L4/L5) per mouse and 5 to 8 sections per DRG tissue (at 80-µm intervals) were immunostained. Briefly, sections were incubated at 4°C overnight with the following mixtures of primary antisera: (1) TRPV1:PAP, (2) A1R:PAP, (3) TRPV1:A1R, and (4) TRPV1:AMPK. Subsequently, the sections were incubated with a combination of Texas red- and fluorescein isothiocyanate-conjugated secondary antisera (1:100; Jackson ImmunoResearch, West Grove, PA) that corresponded to the appropriate primary antisera for 1 hour. Sections after immunofluorescence staining were mounted with Vectashield (Vector, Burlingame, CA) for quantification.

### 2.5. Prostatic acid phosphatase histochemistry

We performed AMP histochemistry with DRG sections to examine PAP ectonucleotidase activity in accordance with previous publications.<sup>35,47</sup> Briefly, the DRG sections were washed twice with 40 mM Trizma-maleate (TM) buffer (pH 5.6) and washed once with 8% sucrose (wt/vol) in TM. The sections were then incubated with substrate solution (3 mM AMP, 2.4 mM lead nitrate, and 8% sucrose in TM) at 37°C for 2 hours. After incubation, the sections were washed 3 times with TM, developed for 10 seconds with 1% sodium sulfide, and then washed 3 times with 0.1 M PB. The sections were finally mounted for quantification.

### 2.6. Quantification of dorsal root ganglion neurons with different phenotypes

To quantify DRG neurons with different phenotypes, each DRG section was systematically photographed at 200× under a fluorescence microscope (Axiophot; Zeiss, Oberkochen, Germany) by following an established procedure to produce a montage of the entire DRG section.<sup>12,13,18</sup> To prevent a density bias, only neurons with a clear nuclear profile were counted, and the areas that contained only neuronal ganglia were measured with Image J ver. 1.44d software (National Institutes of Health, Bethesda, MD). For PAP and A1R morphometric analyses, the neuronal diameters were measured with Image Pro-Plus software (Media Cybernetics, Bethesda, MD) and plotted in histograms.

### 2.7. Measurement of adenosine and adenosine monophosphate with high-performance liquid chromatography analysis

High-performance liquid chromatography (HPLC) was performed to evaluate the efficacy of PAP ectonucleotidase activity after RTX neuropathy developed. The L4/L5 DRG neurons were carefully dissected, and the adenosine and AMP of the neurons were extracted according to our previous protocol.<sup>18</sup> Briefly, the DRG tissues were immersed in 60 µL of sterilized distilled water in an

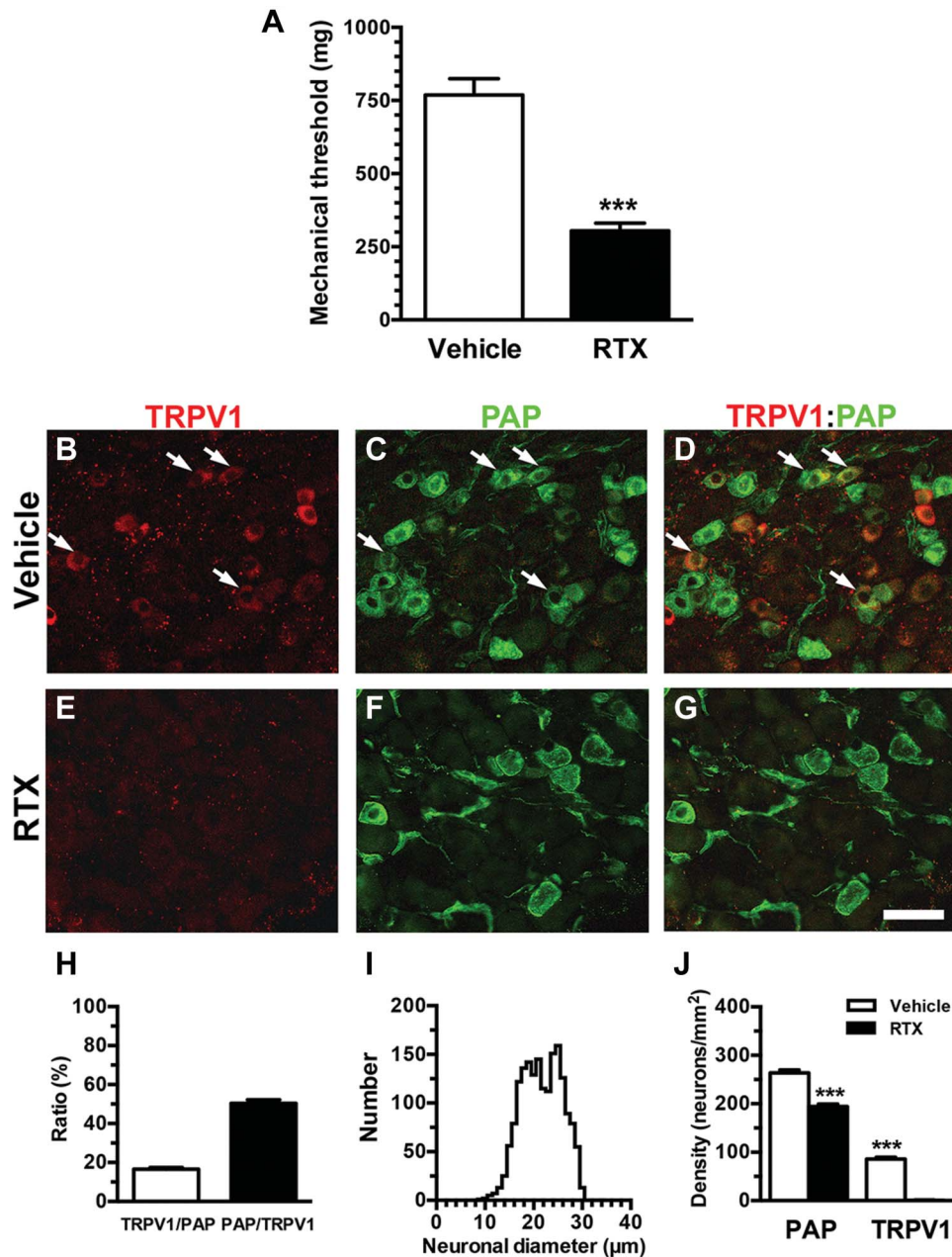


**Figure 1.** Characterization of neuropathic pain hypersensitivity and expression of prostatic acid phosphatase (PAP) and transient receptor potential vanilloid subtype 1 (TRPV1) after resiniferatoxin (RTX) neuropathy. (A) The mechanical threshold was assessed through von Frey monofilament tests using up-and-down algorithms. The graph presents a comparison of the mechanical threshold between the vehicle group (open bar,  $n = 8$ ) and day 7 after RTX neuropathy (RTX group; filled bar,  $n = 6$ ). The mechanical threshold was reduced in RTX neuropathy. (B–G) Double-labeling immunofluorescence staining was performed with anti-TRPV1 (B, D, E, and G in red) and anti-PAP (C, D, F, and G in green) antisera in the dorsal root ganglion (DRG) of vehicle group (B–D) and RTX group (E–G). (D and G) The images show the colocalization patterns of TRPV1 and PAP DRG neurons in the vehicle (D) and RTX (G) groups. Arrow indicated the colocalization of TRPV1 and PAP-expression DRG neurons. (H) The graph indicates the colocalization ratios of TRPV1(+)/PAP(+) (open bar,  $n = 5$ ) and PAP(+)/TRPV1(+) neurons (filled bar,  $n = 5$ ) in the vehicle group according to (B–D). (I) This graph shows the histogram of diameters for PAP(+) neurons in the vehicle group (solid line,  $n = 1761$  neurons). (J) The graphs show density changes in TRPV1(+) neurons and PAP(+) neurons in the vehicle (open bar,  $n = 8$ ) and RTX groups (filled bar,  $n = 8$ ). Bar, 50  $\mu\text{m}$ . \*\*\* $P < 0.001$ .

ultrasonic bath for 15 minutes. After the ultrasonic bath, the samples were filtered with a 0.22- $\mu\text{m}$  syringe filter and separated with a reversed-phase HPLC system.<sup>45</sup> This HPLC system consisted of a photodiode array detector (SPD-M20A; Shimadzu, Kyoto, Japan), binary gradient pumps (LC-20AD XR, Shimadzu), and a manual injector with a 20- $\mu\text{L}$  injection valve. A Brownlee SPP HPLC column (C18, 2.7  $\mu\text{m}$ , 4.6  $\times$  150 mm; PerkinElmer, Waltham, MA) protected with a guard cartridge (C18, 2.7  $\mu\text{m}$ , 4.6  $\times$  5 mm; PerkinElmer) was used in this assay. The mobile phase consisted of potassium

phosphate buffer as buffer A (composed of 39 mM  $\text{K}_2\text{HPO}_4$  and 26 mM  $\text{KH}_2\text{PO}_4$ , adjusted to pH 5.7 with phosphoric acid) and 100% methanol (HPLC grade) as buffer B. Buffer A was prepared with ultrapure water ( $>17.2 \text{ M}\Omega$ ) and filtered with a 0.22- $\mu\text{m}$  filter before use. Before each sample was analyzed, the column was equilibrated with 10 column volumes of buffer A, and then analytical separation was performed. The flow rate was 1 mL/minute, and the gradient profile was as follows: 1 minute at 100% buffer A, 3 minutes at 92.5% buffer A, 7.5 minutes at 80% buffer A, and 10 to 13 minutes at 75%

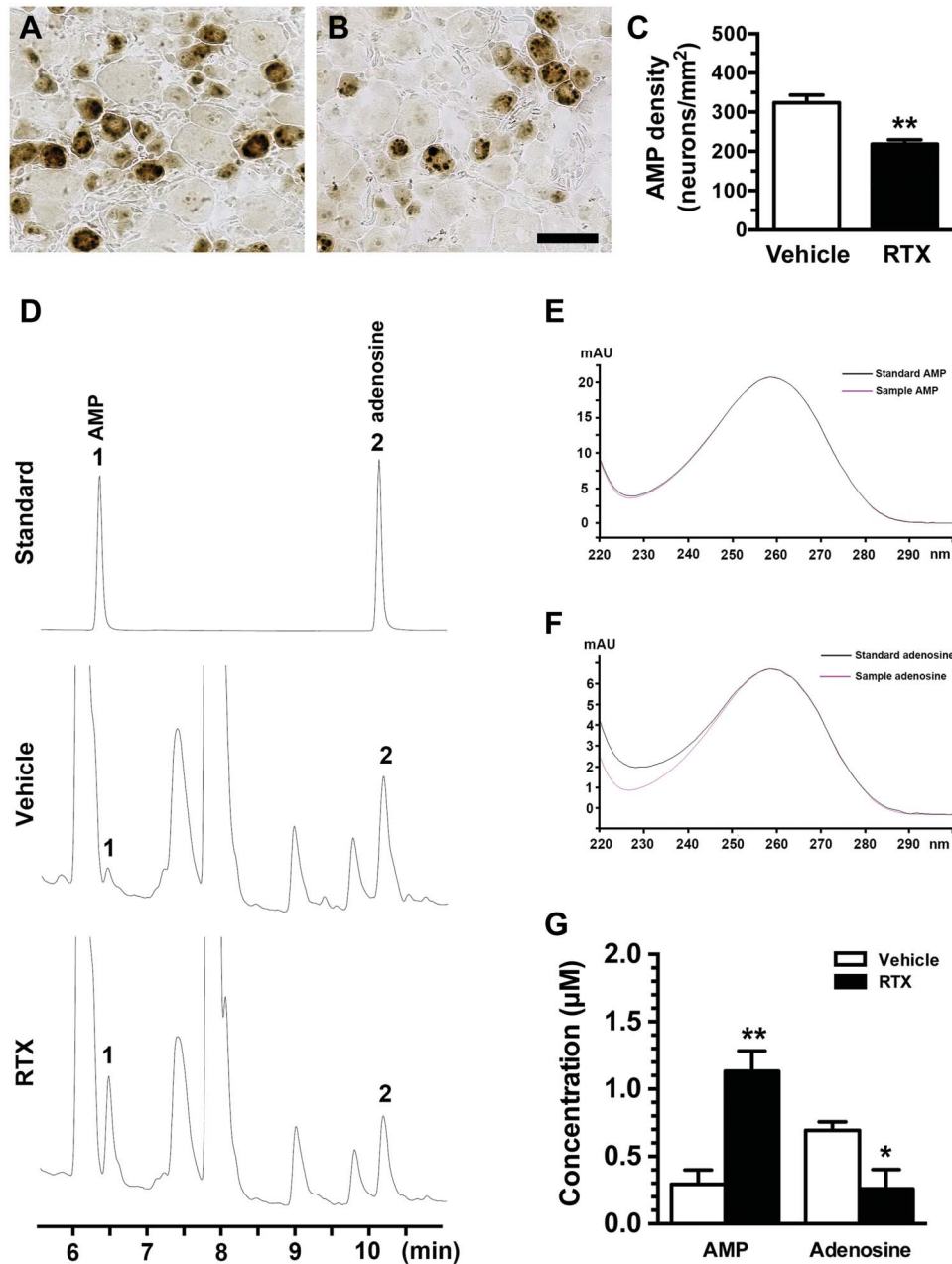


**Figure 2.** Changes in prostatic acid phosphatase (PAP) ectonucleotidase activity and alterations of adenosine hydrolysis in resiniferatoxin (RTX) neuropathy. (A–C) Prostatic acid phosphatase ectonucleotidase activity was assessed through enzyme histochemistry using adenosine monophosphate (AMP, 3 mM) as a substrate. The reaction product was developed with 1% sodium sulfide and appeared dark brown in the dorsal root ganglion (DRG) sections of the vehicle (A) and day 7 after RTX neuropathy (RTX group) (B). (C) The graph shows AMP(+) neuronal densities in the vehicle (open bar,  $n = 5$ ) and RTX (filled bar,  $n = 5$ ) groups according to (A and B). (D–G) High-performance liquid chromatography (HPLC) was conducted to assess the change in the contents of adenosine and AMP, which were extracted from DRG. (D) This graph shows the HPLC chromatograms of the eluted standards (upper panel; AMP, 6.5 minutes; adenosine, 10.2 minutes), the vehicle group (middle panel), and the RTX group (bottom panel). Number designation on the chromatograms: 1 for AMP and 2 for adenosine. (E and F) These figures provide verification of the peaks for AMP (E) and adenosine (F) samples extracted from DRG tissues with respect to a spectral library. The absorbance spectra of the adenosine and AMP samples (pink line in E and F) were the same as the absorbance spectra of the adenosine standard (similarity index = 0.99) and the AMP standard (similarity index = 1.00) (black line in E and F). (G) A significant difference in adenosine signaling molecules was present between the vehicle (open bar,  $n = 6$ ) and RTX groups (filled bar,  $n = 5$ ) (ie, decreased adenosine and increased AMP). Elution time scale, minutes. \* $P < 0.05$ , \*\* $P < 0.01$ . Bar, 50  $\mu\text{m}$ .

buffer A. The concentration of buffer A was returned to 100% at 20 minutes, and the procedure continued for an additional 10 minutes to ensure complete analytical separation and column balance. A single run of analytical separation was terminated at 30 minutes. Chromatograms of adenosine and AMP were obtained at a UV wavelength of 259 nm, and the concentrations of adenosine and AMP were derived from the eluted standards.

## 2.8. Pharmacological interventions of A1Rs and prostatic acid phosphatase through lumbar puncture

Pharmacological studies were conducted to investigate the roles of A1Rs and PAP in analgesic effects. There is significant sequence homology between mouse and human PAP (hPAP),<sup>17</sup> and the analgesic effect of PAP was documented on PAP<sup>-/-</sup> mice.<sup>34,47</sup> In brief, the purified hPAP (EMD

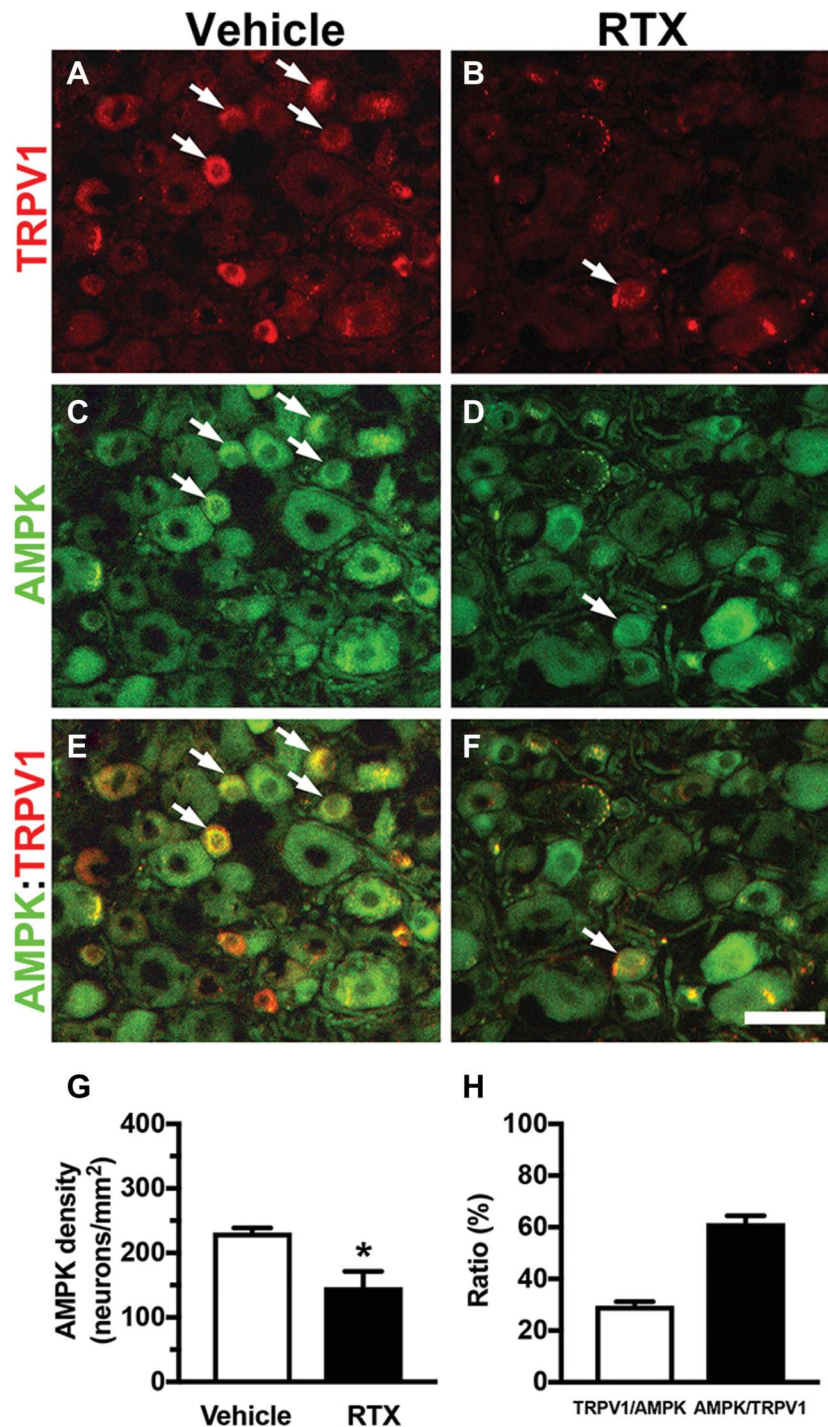


**Figure 3.** Characterization of neuropathic pain hypersensitivity and expression of adenosine monophosphate-activated protein kinase (AMPK) and transient receptor potential vanilloid subtype 1 (TRPV1) after resiniferatoxin (RTX) neuropathy. (A–F) Double-labeling immunofluorescence staining was performed with anti-TRPV1 (A, C, and E in red) and anti-AMPK (B, D, and F in green) antisera in the dorsal root ganglion (DRG) of vehicle group (A and B) and day 7 after RTX neuropathy (RTX group) (C and D). (E and F) The images show the colocalization patterns of TRPV1 and AMPK DRG neurons in the vehicle (G) and RTX (H) groups. Arrow indicated the colocalization of TRPV1 and AMPK expression DRG neurons. (G) The graphs show density changes of AMPK(+) neurons in the vehicle (open bar,  $n = 5$ ) and RTX groups (filled bar,  $n = 5$ ). (H) The graph indicates the colocalization ratios of TRPV1(+)/AMPK(+) (open bar,  $n = 5$ ) and AMPK(+)/TRPV1(+) neurons (filled bar,  $n = 5$ ) in the vehicle group according to (A and C). Bar, 50  $\mu\text{m}$ . \*\* $P < 0.001$ .

Millipore, Temecula, CA) was diluted with normal saline and administered through the i.p. (dose: 9 U) or lumbar puncture route (i.t., dose: 0.3, 3, 9 U) underneath the awake condition. For i.t. lumbar puncture injections, drugs were prepared fresh, diluted with normal saline, and delivered through lumbar puncture (5  $\mu\text{L}$ ) with a Hamilton microsyringe (Hamilton, Reno,

NV)<sup>18</sup> at day 7 of RTX neuropathy (RTXd7). The i.t. lumbar puncture was performed at the level of the intervertebral space between the L4 and L5 vertebrae where L4/L5 DRG are located.<sup>6,18</sup> The control group received normal saline (sham group). To evaluate the PAP effect, changes in the mechanical threshold were assessed at 1 hour (h1), 2 hours (h2), 4 hours

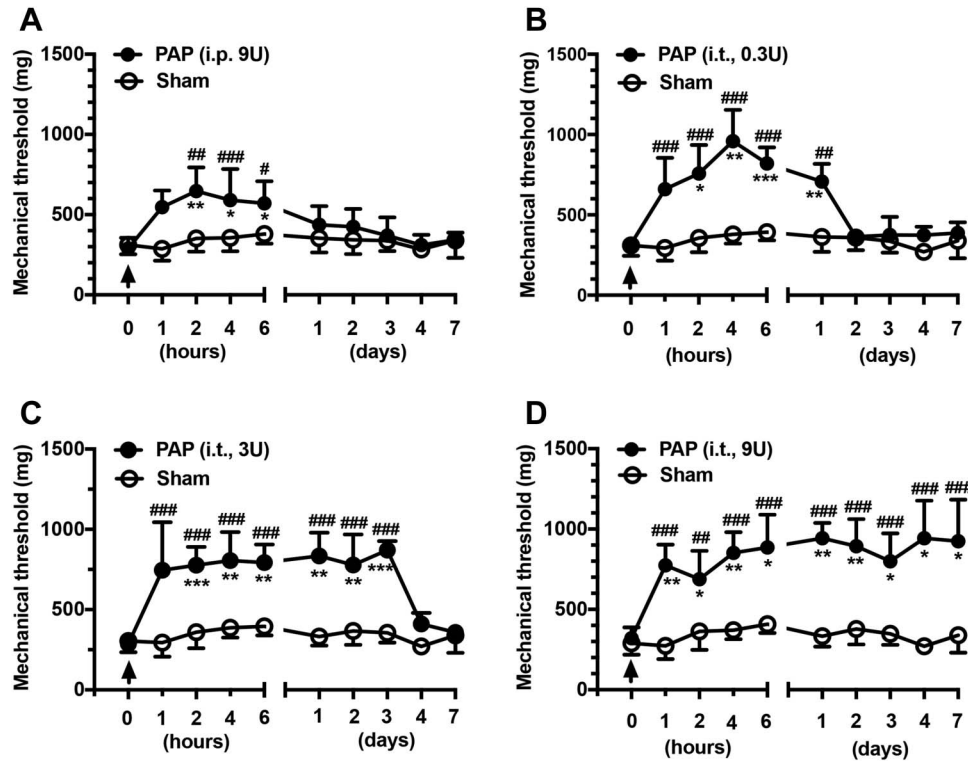


**Figure 4.** Effects of exogenous prostatic acid phosphatase (PAP) on the mechanical threshold in resiniferatoxin (RTX) neuropathy. (A–D) Prostatic acid phosphatase was replenished with purified human PAP (hPAP) administered through either the intraperitoneal (i.p.) injection (A) or intrathecal (i.t.) lumbar puncture (B–D) route in different bioactive doses. The arrow indicates the time point of hPAP administration. The effect of hPAP on the mechanical threshold was examined through von Frey monofilament tests using up-and-down algorithms at 1 hour (h1), 2 hours (h2), 4 hours (h4), 6 hours (h6), 1 day (D1), 2 days (D2), 3 days (D3), 4 days (D4), and 7 days (D7) after hPAP administration. (A) The diagram illustrates the effects of 9 U of hPAP on the mechanical threshold (filled circle,  $n = 6$ ) in comparison with those of saline treatment (sham group; open circle,  $n = 8$ ) through the i.p. route. (B–D) The graphs show the analgesic effects of hPAP administered at doses of 0.3 U (B,  $n = 5$ ), 3 U (C,  $n = 6$ ), and 9 U (D,  $n = 5$ ) through the i.t. route in RTX neuropathy (filled circle) in comparison with sham group (open circle,  $n = 6$ ). \* $P < 0.05$ , \*\* $P < 0.01$ , and \*\*\* $P < 0.001$ : pairing repeated-measures ANOVA followed the Bonferroni post hoc test comparing values before and after hPAP administration. # $P < 0.05$ , ## $P < 0.01$ , and ### $P < 0.001$ : nonpairing repeated-measures ANOVA followed the Bonferroni post hoc test between hPAP and sham group. ANOVA, analysis of variance.

(h4), 6 hours (h6), 1 day (D1), 2 days (D2), 3 days (D3), 4 days (D4), and 7 days (D7) after PAP administration.

A1R pharmacological interventions consisted of (1) A1Rs activated by adenosine (Sigma; dose: 5, 25, 50 nmol), (2) A1Rs antagonized with 8-cyclopentyl-1,3-dipropylxanthine (DPCPX; a selective A1R antagonist, Tocris Bioscience, Bristol, United Kingdom, dose: 10 nmol),<sup>33,35</sup> and (3) DPCPX (10 nmol) 15 minutes before adenosine administration (50 nmol). The mechanical threshold was evaluated at h1, h2, h3, h6, and h24 after the administration of drugs.

## 2.9. Experimental design and statistical analysis

This study examined 2 main topics: (1) PAP expression and its ectonucleotidase activity and products, and (2) pharmacological interventions altering A1Rs and PAP expression. Resiniferatoxin neuropathy is a well-established model of mice of small-fiber neuropathy, which induced the mechanical allodynia at RTXd7 and persisted to RTXd56.<sup>12</sup> The evaluated time point of each approach experiment was at RTXd7, and each group consisted of 5 to 8 mice. Animal was randomized grouping and the coding information was masked during the behavioral tests and quantification procedures. All data are expressed as the mean  $\pm$  SD, and  $t$  tests were performed on data with a Gaussian distribution. For data that did not follow a Gaussian distribution, a nonparametric Mann–Whitney test was conducted. For pharmacological interventions, paired  $t$  tests were performed, and  $P < 0.05$  was considered statistically significant. For

pharmacological study, the 1-way repeated-measures analysis of variances (ANOVAs) were performed followed by the Bonferroni post hoc test when  $P < 0.05$  was obtained.

## 3. Results

### 3.1. Mechanical allodynia and prostatic acid phosphatase expression in resiniferatoxin neuropathy

To characterize neuropathic pain behavioral patterns and PAP expression, we measured the mechanical threshold and performed immunohistochemistry on DRG neurons. The mice in the RTX group showed mechanical allodynia with a reduced mechanical threshold compared with the vehicle group ( $304.4 \pm 64.2$  vs  $769.1 \pm 157.3$  mg,  $P < 0.001$ ) (Fig. 1A). Prostatic acid phosphatase and TRPV1 were coexpressed in some DRG neurons (Figs. 1B–G) with a TRPV1/PAP ratio of  $16.5\% \pm 1.6\%$  and a PAP/TRPV1 ratio of  $50.3\% \pm 3.2\%$  (Fig. 1H). Further analyses showed that PAP(+) neurons were small to medium sized (neuronal diameter of the 25th–75th percentiles:  $18.4$ – $24.9$   $\mu\text{m}$ , Fig. 1I). TRPV1(+) neurons were completely depleted in the RTX group ( $0.8 \pm 1.2$  vs  $81.7 \pm 11.4$  neurons/ $\text{mm}^2$ ,  $P < 0.001$ ), and coexpression of TRPV1 and PAP provided the basis for PAP depletion; ie, the RTX group exhibited a 27% reduction of PAP(+) neurons compared with the vehicle group ( $194.2 \pm 15.2$  vs  $263.8 \pm 18.2$  neurons/ $\text{mm}^2$ ,  $P = 0.0002$ , Fig. 1J).

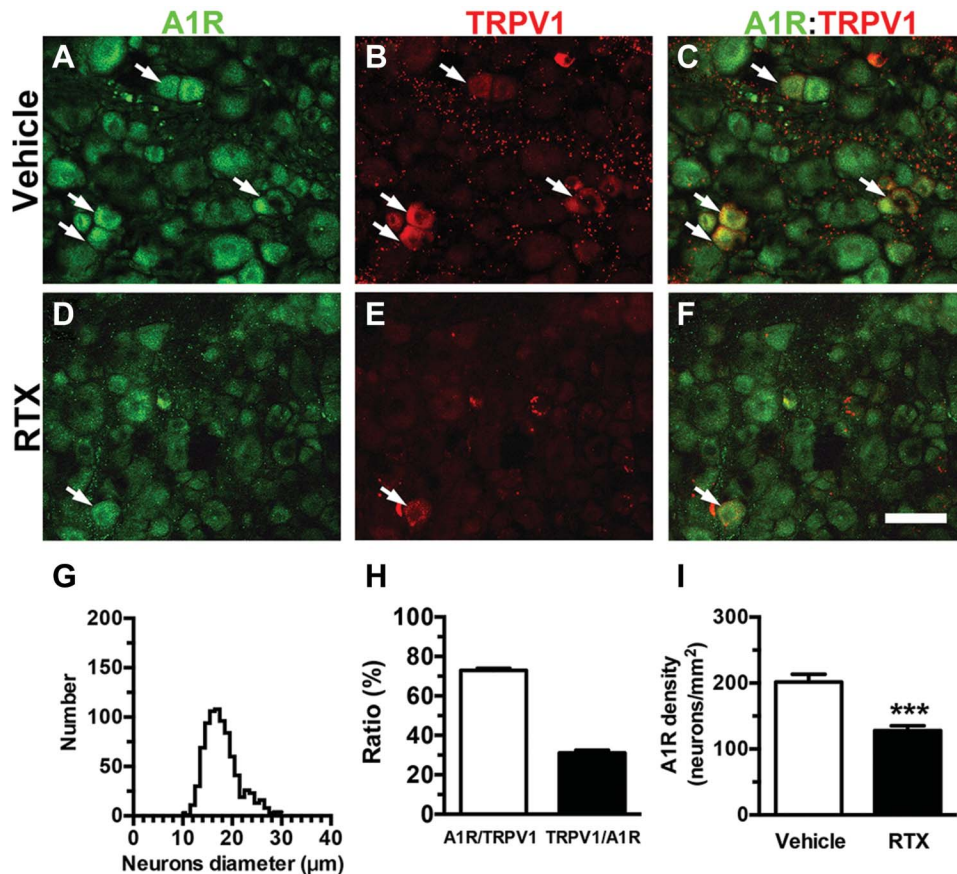


**Figure 5.** Expression of adenosine A1 receptors (A1Rs) in resiniferatoxin (RTX) neuropathy. (A–F) Double-labeling immunofluorescence staining was performed on dorsal root ganglion (DRG) sections with anti-A1R (A, C, D, and F in green) and anti-transient receptor potential vanilloid subtype 1 (TRPV1; B, C, E, and F in red) antisera in the vehicle (A–C) and day 7 after RTX neuropathy (RTX group) (D–F). (C and F) The images show the colocalization of A1R and TRPV1 DRG neurons in the vehicle (C) and RTX (F) groups. Arrow indicated the colocalization of A1R and TRPV1 expression DRG neurons. (G) The graph shows the histogram of diameters for A1R(+) neurons in the vehicle group ( $n = 819$  neurons). (H) The diagram indicates the ratios of A1R(+)/TRPV1(+) (open bar,  $n = 5$ ) and TRPV1(+)/A1R(+) (filled bar,  $n = 5$ ) in the vehicle group in (A–F). (I) The graph shows the density changes in A1R(+) neurons in the vehicle (open bar,  $n = 10$ ) and RTX (filled bar,  $n = 7$ ) groups. \*\*\* $P < 0.001$ . Bar, 50  $\mu\text{m}$ .

### 3.2. Effects of reduced prostatic acid phosphatase expression on adenosine signaling molecules in resiniferatoxin neuropathy

To investigate the effect of PAP expression on functional alterations, we examined PAP ectonucleotidase activity by using AMP histochemistry and HPLC analyses. Adenosine monophosphate is the substrate of PAP ectonucleotidase, and AMP histochemical studies showed a pattern similar to that observed in PAP immunohistochemistry, ie, a reduction in AMP(+) neurons in the RTX group compared with the vehicle group ( $218.2 \pm 25.9$  vs  $323.1 \pm 39.9$  neurons/ $\text{mm}^2$ ,  $P = 0.006$ , **Figs. 2A–C**).

We then performed HPLC to examine the biochemical profiles of PAP ectonucleotidase activity according to the contents of adenosine and AMP in DRG tissues. The eluted AMP (6.5 minutes) and adenosine (10.2 minutes) in the vehicle and RTX groups had the same retention time profiles (**Fig. 2D**) and absorbance spectra (**Figs. 2E and F**) as the standards. The eluted HPLC profiles showed an increased AMP peak ( $1.13 \pm 0.30$  vs  $0.29 \pm 0.26$   $\mu\text{M}$ ,  $P = 0.0015$ ) and a decreased adenosine peak ( $0.26 \pm 0.31$  vs  $0.69 \pm 0.15$   $\mu\text{M}$ ,  $P = 0.016$ ) in the RTX group compared with the vehicle group (**Fig. 2G**). We further investigated the profiles of AMPK that was activated by AMP,<sup>10</sup> which also had analgesic effect.<sup>19,25</sup> Adenosine monophosphate-activated PK was reduced by RTX with a 35% reduction ( $231.8 \pm 14.1$  vs  $147.0 \pm 55.0$  neurons/ $\text{mm}^2$ ,

$P = 0.021$ ) which was related to colocalization with TRPV1 [30% of TRPV1(+)/AMPK(+) and 62% of AMPK(+)/TRPV1(+)] (**Fig. 3**). Collectively, the decrease in PAP expression resulted in reduced adenosine ligand in adenosine signaling was a major effector leading to dysfunction of cellular analgesia.

### 3.3. Reversal of mechanical allodynia in resiniferatoxin neuropathy by exogenous prostatic acid phosphatase

To further confirm the analgesic effect of PAP, bioactive hPAP was administered at RTXd7 using both the i.p. and i.t. routes. Before hPAP administration, the mice showed mechanical allodynia ( $P < 0.001$ ) at RTXd7 (**Fig. 4**). Treatment with hPAP through the i.p. route (dose: 9 U) had mild analgesic effects, namely a partial reversal of the reduced mechanical threshold at h2 compared with the mechanical threshold at RTXd7 ( $646.4 \pm 148.1$  vs  $288.8 \pm 66.8$  mg,  $P < 0.01$ , repeated-measures 1-way ANOVA), and this status lasted until h6 ( $570.6 \pm 137.7$  mg,  $P < 0.05$ , **Fig. 4A**). Notably, hPAP administered using the i.t. route exhibited a higher efficacy and longer duration of analgesic effects than that administered using the i.p. route. Furthermore, i.t. administration of hPAP resulted in a dose-dependent reduction of mechanical allodynia. For example, the mechanical threshold was normalized from h2 ( $758.0 \pm 177.2$  vs  $319.1 \pm 41.6$  mg) to D1 ( $708.4 \pm 109.8$  mg,  $P < 0.01$ ) at 0.3 U (**Fig. 4B**). At the 3 U dose, the analgesic effect lasted from h2

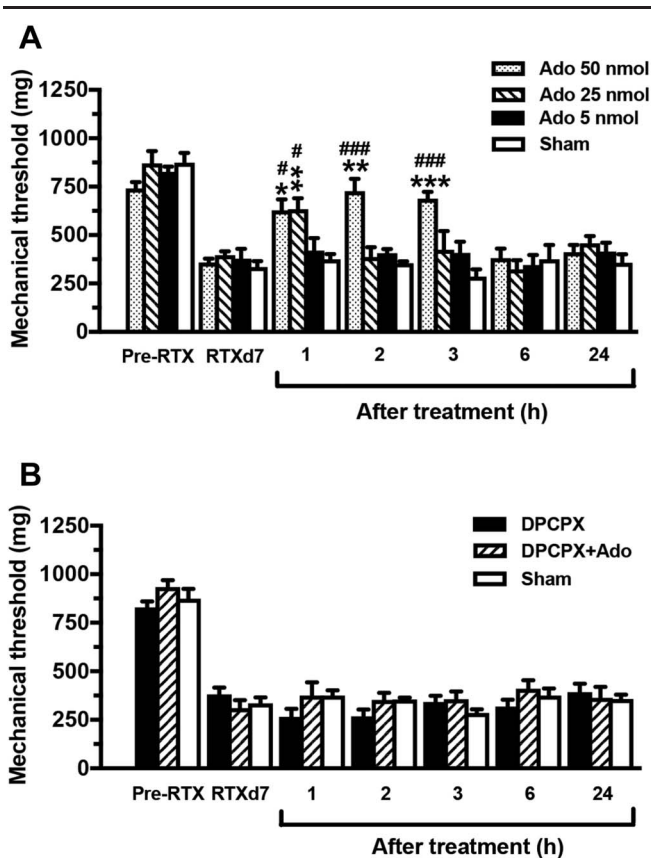


**Figure 6.** Pharmacological interventions altering adenosine A1 receptors (A1Rs) expression in resiniferatoxin (RTX) neuropathy. Pharmacological interventions of A1Rs were conducted with (1) an A1R agonist (adenosine, Ado;  $n = 5$ ), (2) A1R antagonist (8-cyclopentyl-1,3-dipropylxanthine [DPCPX],  $n = 6$ ) after adenosine, and (3) DPCPX ( $n = 5$ ) administration through intrathecal lumbar puncture at day 7 after RTX neuropathy (RTXd7). The mechanical threshold was evaluated through the von Frey monofilament test at 1 hour (h1), 2 hours (h2), 3 hours (h3), 6 hours (h6), and 24 hours (h24) after drug administration. (A) The graph indicates the changes in the mechanical threshold in RTX neuropathy after adenosine treatment at doses of 50 (dotted bar), 25 (slashed bar), and 5 nmol (filled bar). The analgesic effect of adenosine was dose-dependent, but that of saline treatment (sham group) was not (unfilled bar). (B) The graph indicates the antagonistic effect of DPCPX (10 nmol) after the administration of adenosine (50 nmol) on mechanical thresholds in RTX neuropathy. DPCPX blocked the analgesic effect of adenosine. \* $P < 0.05$ , \*\* $P < 0.01$ , and \*\*\* $P < 0.001$ : pairing repeated-measures ANOVA followed the Bonferroni post hoc test comparing values before and after administration of adenosine. # $P < 0.05$  and ### $P < 0.001$ : nonpairing repeated-measures ANOVA followed the Bonferroni post hoc test between adenosine and sham treatments. ANOVA, analysis of variance.

(776.5  $\pm$  113.5 vs 287.0  $\pm$  44.5 mg,  $P < 0.001$ ) to D3 (871.1  $\pm$  57.2 mg,  $P < 0.001$ ; **Fig. 4C**). The 9 U dose had the highest efficacy in producing an analgesic effect from h1 (774.4  $\pm$  129.2 vs 320.8  $\pm$  68.3 mg,  $P < 0.01$ ) to D7 (924.8  $\pm$  259.1 mg,  $P < 0.05$ ; **Fig. 4D**). These results indicated that replenishment of bioactive hPAP compensated for changes in the mechanical threshold due to PAP depletion.

### 3.4. Effect of resiniferatoxin on A1Rs

To determine whether RTX also affected the adenosine receptor, we examined A1R expression in RTX neuropathy (**Fig. 5**). A1R(+) neurons belonged to the category of small-diameter neurons (diameter of the 25th–75th percentiles: 15.5–19.7  $\mu\text{m}$ , **Fig. 5G**). The colocalization ratio of A1R and TRPV1 was approximately 73% in A1R(+)/TRPV1(+) neurons, and approximately 30% of

the A1R(+) neurons also expressed TRPV1 in the vehicle group (**Figs. 5C, F, and H**). This colocalization ratio provided the basis for an approximately 34% reduction in A1R(+) neurons (127.9  $\pm$  19.8 vs 193.1  $\pm$  22.4 neurons/ $\text{mm}^2$ ;  $P < 0.001$ , **Fig. 5I**).

To determine the functional significance of A1R reduction in RTX neuropathy, adenosine (as an A1R agonist) and DPCPX (as an A1R antagonist) were administered through an i.t. lumbar route with different protocols to examine the changes in neuropathic pain hypersensitivity (**Fig. 6**). Before adenosine administration, the mice showed mechanical allodynia ( $P < 0.001$ ) at RTXd7. At the 50 nmol dose, pain hypersensitivity was alleviated at h1 (627.5  $\pm$  140.7 vs 357.9  $\pm$  50.1 mg,  $P < 0.05$ , repeated-measures 1-way ANOVA), and this alleviation lasted until h3 (688.2  $\pm$  85.3 mg,  $P < 0.001$ ). Allodynia reappeared at h6 with a mechanical threshold similar to that of the sham group (334.9  $\pm$  60.7 mg,  $P > 0.05$ ). The pain hypersensitivity-relief effect induced by adenosine was dose dependent: the relief of mechanical allodynia became obvious after the 25 nmol dose at h1 (633.5  $\pm$  126.9 vs 395.6  $\pm$  46.2 mg,  $P < 0.01$ ), and mechanical allodynia returned at h2 (386.8  $\pm$  112.9 mg,  $P > 0.05$ ). Injection at the 5 nmol dose had no effect on the mechanical threshold ( $P > 0.05$ ). By contrast, DPCPX blocked the adenosine-mediated analgesia and did not affect the mechanical threshold at any time point (**Fig. 6B**).

### 3.5. A1R(+):PAP(+) neurons are responsible for the pain hypersensitivity in resiniferatoxin neuropathy

To examine the influence of A1Rs and PAP coexpression on neuropathic pain hypersensitivity behaviors, we analyzed mechanical thresholds in the context of colocalization. Double-labeling studies showed that approximately 50% of A1R(+) and PAP(+) neurons were colocalized (ie, 48.5%  $\pm$  6.9% of A1R(+)/PAP(+) and 59.7%  $\pm$  9.9% of PAP(+)/A1R(+) neurons, **Figures 7A–G**). Regression analyses indicated that the PAP(+) ( $r = 0.74$ ,  $P = 0.0009$ ; **Fig. 7H**) and A1R(+) neuronal densities ( $r = 0.89$ ,  $P = 0.0002$ ; **Fig. 7I**) were linearly correlated with the mechanical threshold. Furthermore, the density of neurons that coexpressed A1Rs and PAP was linearly correlated with the mechanical threshold ( $r = 0.79$ ,  $P = 0.0039$ ), suggesting that A1R(+):PAP(+) neurons are functional cellular analgesic units (**Fig. 7J**). This speculation was confirmed by extracting A1R(+):PAP(+) neurons from either A1R(+) or PAP(+) neurons. Only marginal correlations were present between the A1R(–)/PAP(+) neuronal density and mechanical threshold ( $r = -0.61$ ,  $P = 0.045$ , **Fig. 7K**), and no correlation was evident between the A1R(+)/PAP(–) neuronal density and mechanical threshold ( $r = 0.51$ ,  $P = 0.11$ , **Fig. 7L**). Taken together, these refined analyses indicated that only A1R(+):PAP(+) neurons were linearly correlated with the mechanical threshold and responsible for neuropathic pain hypersensitivity.

## 4. Discussion

This study documents the impaired adenosine analgesia system that underlies neuropathic pain behavior in RTX neuropathy at the levels of the ligand (adenosine) and the receptors (A1Rs), particularly in the A1R(+):PAP(+) neurons.

### 4.1. Reduced prostatic acid phosphatase leading to pain hypersensitivity in resiniferatoxin neuropathy

The reduction of PAP(+) neurons in RTX neuropathy leads to reduced ectonucleotidase activity and hence decreased

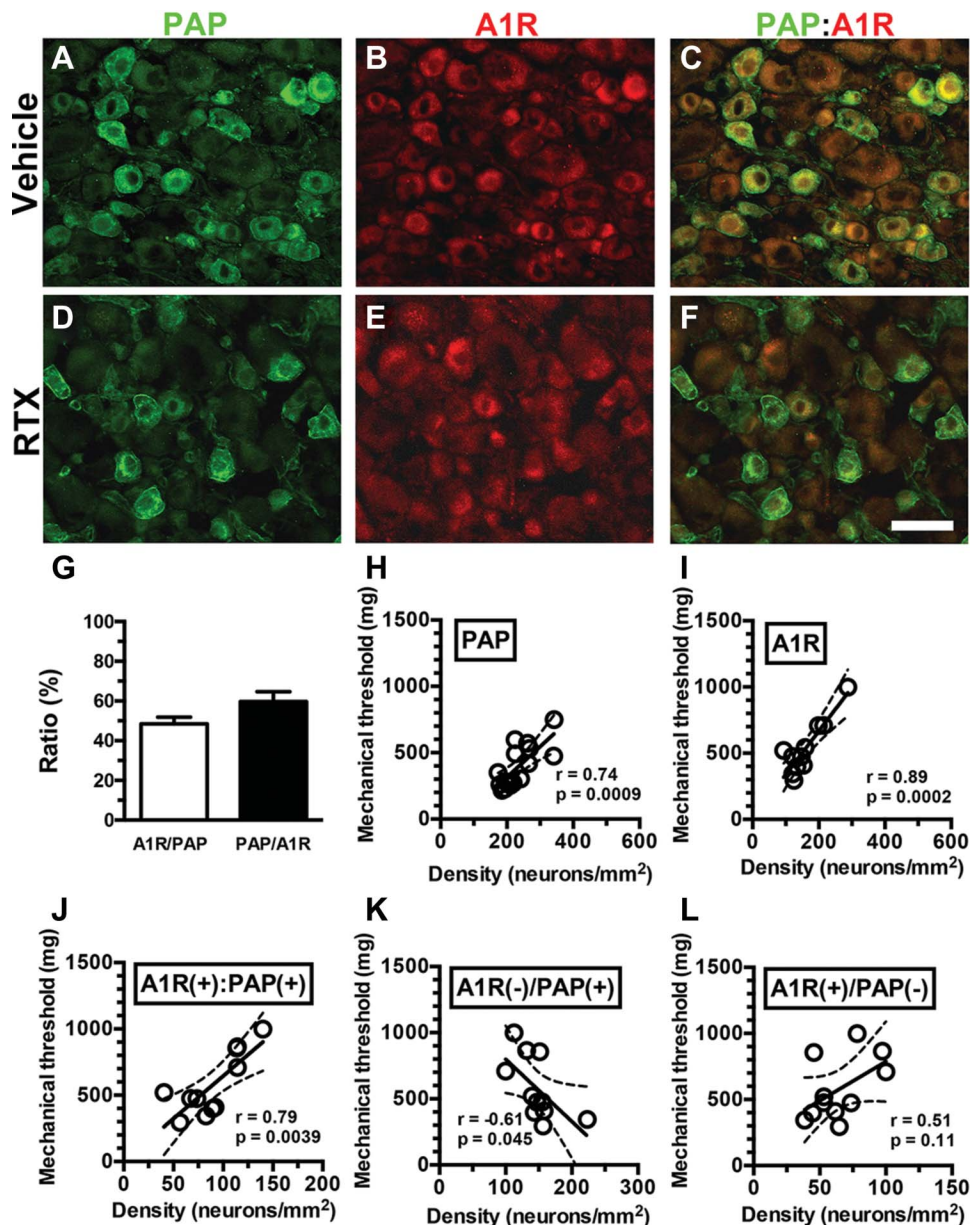


**Figure 7.** Contributions of adenosine A1 receptors (A1Rs) and prostatic acid phosphatase (PAP) neurons to neuropathic pain hypersensitivity in resiniferatoxin (RTX) neuropathy. (A–F) Double-labeling immunofluorescence staining was performed on dorsal root ganglion (DRG) sections with anti-PAP (A, C, D, and F in green) and anti-A1R (B, C, E, and F in red) antisera in the vehicle group (A–C) and day 7 after RTX neuropathy (RTX group; D–F). (C and F) The images show colocalization of A1R and PAP DRG neurons in the vehicle (C) and RTX (F) groups. (G) The diagram indicates the ratios of A1R(+)/PAP(+) (open bar,  $n = 6$ ) and PAP(+)/A1R(+) (filled bar,  $n = 6$ ) in the vehicle group shown in (A–F). (H–L) The mechanical threshold was assessed through von Frey monofilament tests using up-and-down algorithm. The mechanical threshold was highly linearly correlated with the densities of PAP(+) (H,  $n = 16$ ), A1R(+) (I,  $n = 11$ ), and A1R(+):PAP(+) neurons (J,  $n = 11$ ). By contrast, the density of A1R(-)/PAP(+) neurons (K,  $n = 11$ ) showed a weak linear correlation with the mechanical threshold, and no linear correlation between A1R(+)/PAP(-) neurons (L,  $n = 11$ ) and the mechanical threshold was evident. Bar, 50  $\mu\text{m}$ .

adenosine content in DRG neurons, which contributes to the reduction of analgesic signaling at the ligand level. TRPV1(+) neurons were almost depleted in RTX neuropathy, and approximately 17% of PAP(+) neurons were colocalized with TRPV1(+) neurons, which accounted for the susceptibility of PAP(+) neurons to RTX. The finding that PAP(+) neurons were reduced by 27% in RTX neuropathy suggests that additional RTX effects may underlie the downregulation of PAP(+) neurons in RTX neuropathy. The activating transcription factor 3 (ATF3), an neuronal injury and pain marker,<sup>12</sup> was upregulated in remaining PAP(+) neurons, and the number of ATF3(+):PAP(+) neurons was correlated with the degree of neuropathic pain

hypersensitivity.<sup>41</sup> Furthermore, PAP coexpressed with trkA in NGF-dependent nociceptors and NGF replenishment could rescue PAP neurons and normalized neuropathic pain behaviors.<sup>41</sup> Taken together, injured small-sized PAP(+) neurons were the major neurons responsible for the impairment of cellular analgesia, leading to neuropathic pain behaviors.

Prostatic acid phosphatase hydrolyzes extracellular AMP to adenosine as a ligand of adenosine receptors responsible for analgesic effects.<sup>36,43,47</sup> This is supported by our observation that the PAP(+) neuronal density was linearly correlated with the mechanical threshold. In the current study, we further demonstrated the effects of reduced PAP(+) neurons, including (1)

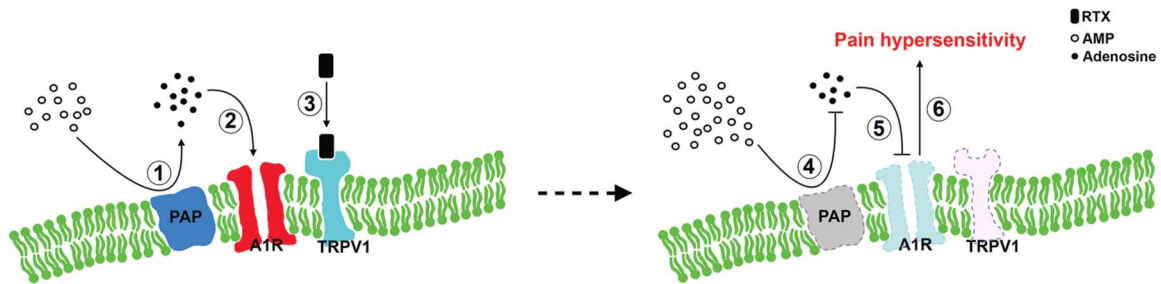


**Figure 8.** Adenosine signaling modulates pain hypersensitivity behaviors in resiniferatoxin (RTX) neuropathy. This diagram shows an analgesia pathway in small-fiber neuropathy: (left panel) membrane-bound PAP hydrolyzes AMP into adenosine (1) which activates A1Rs as the cellular analgesia mechanism (2). (3) TRPV1 coexpressed with PAP and A1Rs, and TRPV1 were depleted by RTX, causes a decrease in analgesic adenosine signaling, including a reduction in PAP ectonucleotidase activity and A1Rs depletion (dotted profiles in right panel). The reduced PAP ectonucleotidase activity causes a decrease in extracellular AMP hydrolysis (4), which results in a reduction in adenosine. (5) A parallel reduction of A1R(+) leads to the disability of adenosine signaling and further exacerbates the development of pain hypersensitivity (6). A1R, adenosine A1 receptor; AMP, adenosine monophosphate; PAP, prostatic acid phosphatase; TRPV1, transient receptor potential vanilloid type 1.

reduced AMP(+) neurons on AMP histochemistry and (2) reduced AMP hydrolysis to adenosine in DRG neurons on HPLC, which led to impaired adenosine signaling. Paradoxically, AMP also had the analgesic effect<sup>9,15</sup> by acting as an agonist of A1Rs,<sup>26</sup> and AMP activates AMPK,<sup>10</sup> which consequentially phosphorylated AMPK and reversed pain hypersensitivity<sup>19,25,29</sup> such as in the diabetic neuropathy.<sup>11,29</sup> The increase in AMP by the reduction of PAP ectonucleotidase activity did not exert effects in RTX neuropathy model. The current study demonstrated that both AMPK and A1Rs were coexpressed with TRPV1, which were also depleted by RTX. This line evidence may explain the absence of analgesic effect by AMP. Together, these observations provide evidence of the downregulated PAP cellular analgesic mechanisms that underlie the pain hypersensitivity in nerve-degeneration-induced small-fiber neuropathy.

#### 4.2. Effects of resiniferatoxin neuropathy on A1Rs in analgesic signaling

This study further demonstrated that downregulation of A1Rs and the decreased generation of the ligand, adenosine, due to decreased PAP expression are responsible for the pain hypersensitivity in RTX neuropathy. Previously, studies examining the molecular mechanisms of neuropathic pain mainly focused on the pronociceptive system, including the purinergic receptors<sup>12</sup> and proinflammatory molecules.<sup>8</sup> This study indicates that the receptor involved in cellular analgesia is downregulated and contributes to the pain hypersensitivity in RTX neuropathy through 2 lines of evidence: (1) downregulation of A1Rs in DRG neurons and (2) pharmacological intervention of A1Rs to reverse neuropathic pain hypersensitivity. The downregulation of A1Rs was attributed to the colocalization of A1R with TRPV1, which is depleted in RTX neuropathy. However, the analgesic effect of A1R activation in adenosine signaling was transient, which might be related to the short half-life of adenosine,<sup>22</sup> indicating that PAP is an upstream regulator of functional adenosine signaling. The long duration of analgesia attained through exogenous PAP replenishment confirmed this speculation.

Adenosine is also an agonist to other phenotypic adenosine receptors.<sup>32</sup> This present report focuses on A1R and demonstrates that A1R is the major downstream receptor underlying PAP cellular analgesia according to (1) antagonism with DPCPX that blocked the analgesic effect of adenosine and (2) the correlation of A1R(+):PAP(+) neuronal densities with the degree of neuropathic pain hypersensitivity. There was ~50%

colocalization ratio of PAP and A1R based on the analysis of immunohistochemical patterns. The results of linear regression analysis suggested that A1R(+):PAP(+) neurons could serve as functional cellular analgesic units acting through an autocrine mechanism<sup>5</sup> (ie, A1R activation is the major effector of adenosine in this RTX neuropathy model). Although this study was focused on A1R, the results do not exclude potential contributions of other adenosine receptors, in particular A3R, to neuropathic pain behaviors in RTX neuropathy. Further studies by applying knockout mice or pharmacological interventions on other phenotypic adenosine receptors are necessary to address this issue.

#### 4.3. Modulation of cellular analgesia by transient receptor potential vanilloid type 1 in resiniferatoxin neuropathy and its clinical implications

Transient receptor potential vanilloid type 1 is a nonselective ion channel and a polymodal nociceptor; in particular, it transmits the thermal nociception<sup>2,3</sup> through an increase in calcium ion influx and altered intracellular signaling.<sup>21,28</sup> The current study demonstrated that depletion of TRPV1 in RTX neuropathy resulted in an impaired cellular analgesia pathway at the ligand (adenosine) and associated receptors (A1R) levels. Prostatic acid phosphatase was mainly expressed in nonpeptidergic neurons and a subset of CGRP(+) neurons.<sup>40</sup> In this study, we documented the colocalization profiles of TRPV1 and PAP, which clarified the role of PAP depletion in RTX neuropathy (Fig. 8). This observation implied that molecular interactions occur between TRPV1 and PAP. Both TRPV1 and PAP are membrane-bound molecules, which raises an intriguing question: Do their interactions through cytoplasm membrane microdomains involve other pronociceptive molecules? For example, PAP results in analgesia by a reduction of TRPV1 activity<sup>34</sup> and growing evidence suggests that TRPV1-mediated nociception requires the integrity of lipid raft microdomains.<sup>20,30,31,38</sup> These reports imply that the imbalance between PAP and TRPV1 leads to the pain hypersensitivity, which may parallel PAP-expression downregulation. Further studies will be required to confirm this speculation.

Finally, a steady state of the extracellular adenosine metabolism is necessary to maintain a balanced cellular analgesic system. Extracellular AMP accumulation may enhance AMPK, a crucial cellular sensor that monitors AMP/ATP and ADP/ATP ratios underlying cellular stress.<sup>10</sup> This current report also demonstrated AMPK downregulation in RTX neuropathy.

Collectively, these observations suggest that both intrinsic and extrinsic molecules alter the balance between analgesic and nociceptive molecules contributing to the development of pain hypersensitivity after systemic nerve injury in RTX neuropathy.

### Conflict of interest statement

The authors have no conflict of interest to declare.

This work was supported by grants from the National Science Council (099-2815-C-037-001-B, 100-2320-B-002-083-MY3, and 102-2321-B-002-061), the Ministry of Science and Technology (103-2320-B-037-015-MY3, 103-2320-B-002-018, and 106-2320-B-037-024), the Translational Medicine Project, National Taiwan University College of Medicine and National Taiwan University Hospital (101C101-201), the Project of Top Competitive Groups, National Taiwan University (106R881001), and the Aim for the Top Universities Grant, Kaohsiung Medical University (KMU-TP104PR19 and TP105PR15), and from Chi-Mei Medical Center and Kaohsiung Medical University Research Foundation (106CM-KMU-04).

### Article history:

Received 3 January 2018

Received in revised form 6 April 2018

Accepted 11 April 2018

Available online 16 April 2018

### References

- Antonioli L, Blandizzi C, Pacher P, Hasko G. Immunity, inflammation and cancer: a leading role for adenosine. *Nat Rev Cancer* 2013;13:842–57.
- Caterina MJ, Leffler A, Malmberg AB, Martin WJ, Trafton J, Petersen-Zeitl KR, Koltzenburg M, Basbaum AI, Julius D. Impaired nociception and pain sensation in mice lacking the capsaicin receptor. *Science* 2000;288:306–13.
- Caterina MJ, Schumacher MA, Tominaga M, Rosen TA, Levine JD, Julius D. The capsaicin receptor: a heat-activated ion channel in the pain pathway. *Nature* 1997;389:816–24.
- Chaplan SR, Bach FW, Pogrel JW, Chung JM, Yaksh TL. Quantitative assessment of tactile allodynia in the rat paw. *J Neurosci Methods* 1994; 53:55–63.
- Dando R, Dvoryanchikov G, Pereira E, Chaudhari N, Roper SD. Adenosine enhances sweet taste through A2B receptors in the taste bud. *J Neurosci* 2012;32:322–30.
- Fairbanks CA. Spinal delivery of analgesics in experimental models of pain and analgesia. *Adv Drug Deliv Rev* 2003;55:1007–41.
- Ferrari LF, Levine JD. Plasma membrane mechanisms in a preclinical rat model of chronic pain. *J Pain* 2015;16:60–6.
- Funahashi Y, Oguchi T, Goins WF, Gotoh M, Tyagi P, Goss JR, Glorioso JC, Yoshimura N. Herpes simplex virus vector mediated gene therapy of tumor necrosis factor- $\alpha$  blockade for bladder overactivity and nociception in rats. *J Urol* 2013;189:366–73.
- Goldman N, Chen M, Fujita T, Xu Q, Peng W, Liu W, Jensen TK, Pei Y, Wang F, Han X, Chen JF, Schnermann J, Takano T, Bekar L, Tieu K, Nedergaard M. Adenosine A1 receptors mediate local anti-nociceptive effects of acupuncture. *Nat Neurosci* 2010;13:883–8.
- Hardie DG, Ross FA, Hawley SA. AMPK: a nutrient and energy sensor that maintains energy homeostasis. *Nat Rev Mol Cell Biol* 2012;13: 251–62.
- Hasanvand A, Amini-Khoei H, Hadian MR, Abdollahi A, Tavangar SM, Dehpour AR, Semiee E, Mehr SE. Anti-inflammatory effect of AMPK signaling pathway in rat model of diabetic neuropathy. *Inflammopharmacology* 2016;24:207–19.
- Hsieh YL, Chiang H, Lue JH, Hsieh ST. P2X3-mediated peripheral sensitization of neuropathic pain in resiniferatoxin-induced neuropathy. *Exp Neurol* 2012;235:316–25.
- Hsieh YL, Chiang H, Tseng TJ, Hsieh ST. Enhancement of cutaneous nerve regeneration by 4-methylcatechol in resiniferatoxin-induced neuropathy. *J Neuropathol Exp Neurol* 2008;67:93–104.
- Hsieh YL, Lin CL, Chiang H, Fu YS, Lue JH, Hsieh ST. Role of peptidergic nerve terminals in the skin: reversal of thermal sensation by calcitonin gene-related peptide in TRPV1-depleted neuropathy. *PLoS One* 2012;7: e50805.
- Hurt JK, Zylka MJ. PAPuncture has localized and long-lasting antinociceptive effects in mouse models of acute and chronic pain. *Mol Pain* 2012;8:28.
- Johansson B, Halldner L, Dunwiddie TV, Masino SA, Poelchen W, Gimenez-Llort L, Escorihuela RM, Fernandez-Teruel A, Wiesenfeld-Hallin Z, Xu XJ, Hardemark A, Betsholtz C, Herlenius E, Fredholm BB. Hyperalgesia, anxiety, and decreased hypoxic neuroprotection in mice lacking the adenosine A1 receptor. *Proc Natl Acad Sci U S A* 2001;98:9407–12.
- Kong HY, Byun J. Emerging roles of human prostatic acid phosphatase. *Biomol Ther (Seoul)* 2013;21:10–20.
- Lin CL, Fu YS, Hsiao TH, Hsieh YL. Enhancement of purinergic signalling by excessive endogenous ATP in resiniferatoxin (RTX) neuropathy. *Purinergic Signal* 2013;9:249–57.
- Maixner DW, Yan X, Gao M, Yadav R, Weng HR. Adenosine monophosphate-activated protein kinase regulates Interleukin-1 $\beta$  expression and glial glutamate transporter function in rodents with neuropathic pain. *Anesthesiology* 2015;122:1401–13.
- Marchenkova A, Vilotti S, Ntamati N, van den Maagdenberg AM, Nistri A. Inefficient constitutive inhibition of P2X3 receptors by brain natriuretic peptide system contributes to sensitization of trigeminal sensory neurons in a genetic mouse model of familial hemiplegic migraine. *Mol Pain* 2016; 12:1–12.
- Moriello AS, De Petrocellis L. Assay of TRPV1 receptor signaling. *Methods Mol Biol* 2016;1412:65–76.
- Moser GH, Schrader J, Deussen A. Turnover of adenosine in plasma of human and dog blood. *Am J Physiol* 1989;256:C799–806.
- Nascimento FP, Macedo-Junior SJ, Pamplona FA, Luiz-Cerutti M, Cordova MM, Constantino L, Tasca CI, Dutra RC, Calixto JB, Reid A, Sawynok J, Santos AR. Adenosine A1 receptor-dependent antinociception induced by inosine in mice: pharmacological, genetic and biochemical aspects. *Mol Neurobiol* 2015;51:1368–78.
- Pan HL, Khan GM, Alloway KD, Chen SR. Resiniferatoxin induces paradoxical changes in thermal and mechanical sensitivities in rats: mechanism of action. *J Neurosci* 2003;23:2911–19.
- Price TJ, Das V, Dussor G. Adenosine monophosphate-activated protein kinase (AMPK) activators for the prevention, treatment and potential reversal of pathological pain. *Curr Drug Targets* 2016;17:908–20.
- Rittiner JE, Korboukh I, Hull-Ryde EA, Jin J, Janzen WP, Frye SV, Zylka MJ. AMP is an adenosine A1 receptor agonist. *J Biol Chem* 2012;287: 5301–9.
- Rivera-Oliver M, Diaz-Rios M. Using caffeine and other adenosine receptor antagonists and agonists as therapeutic tools against neurodegenerative diseases: a review. *Life Sci* 2014;101:1–9.
- Rosenbaum T, Simon SA. TRPV1 receptors and signal transduction. In: Liedtke WB, Heller S, editors. TRP ion channel function in sensory transduction and cellular signaling cascades. Boca Raton, FL: CRC Press/Taylor & Francis, 2007.
- Russe OQ, Moser CV, Kynast KL, King TS, Stephan H, Geisslinger G, Niederberger E. Activation of the AMP-activated protein kinase reduces inflammatory nociception. *J Pain* 2013;14:1330–40.
- Saghy E, Szoke E, Payrits M, Helyes Z, Borzsei R, Erostryak J, Janosi TZ, Setalo G Jr, Szolcsanyi J. Evidence for the role of lipid rafts and sphingomyelin in Ca-gating of transient receptor potential channels in trigeminal sensory neurons and peripheral nerve terminals. *Pharmacol Res* 2015;100:101–16.
- Santha P, Oszlacs O, Dux M, Dobos I, Jancso G. Inhibition of glucosylceramide synthase reversibly decreases the capsaicin-induced activation and TRPV1 expression of cultured dorsal root ganglion neurons. *PAIN* 2010;150:103–12.
- Sawynok J. Adenosine receptor targets for pain. *Neuroscience* 2016; 338:1–18.
- Sawynok J, Reid AR. Caffeine inhibits antinociception by acetaminophen in the formalin test by inhibiting spinal adenosine A(1) receptors. *Eur J Pharmacol* 2012;674:248–54.
- Sowa NA, Street SE, Vihko P, Zylka MJ. Prostatic acid phosphatase reduces thermal sensitivity and chronic pain sensitization by depleting phosphatidylinositol 4,5-bisphosphate. *J Neurosci* 2010;30:10282–93.
- Sowa NA, Vadakkan KI, Zylka MJ. Recombinant mouse PAP has pH-dependent ectonucleotidase activity and acts through A(1)-adenosine receptors to mediate antinociception. *PLoS One* 2009;4:e4248.
- Street SE, Walsh PL, Sowa NA, Taylor-Blake B, Guillot TS, Vihko P, Wightman RM, Zylka MJ. PAP and NT5E inhibit nociceptive neurotransmission by rapidly hydrolyzing nucleotides to adenosine. *Mol Pain* 2011;7:80.
- Street SE, Zylka MJ. Emerging roles for ectonucleotidases in pain-sensing neurons. *Neuropsychopharmacology* 2011;36:358.

- [38] Szoke E, Borzsei R, Toth DM, Lengl O, Helyes Z, Sandor Z, Szolcsanyi J. Effect of lipid raft disruption on TRPV1 receptor activation of trigeminal sensory neurons and transfected cell line. *Eur J Pharmacol* 2010;628:67–74.
- [39] Takano T, Chen X, Luo F, Fujita T, Ren Z, Goldman N, Zhao Y, Markman JD, Nedergaard M. Traditional acupuncture triggers a local increase in adenosine in human subjects. *J Pain* 2012;13:1215–23.
- [40] Taylor-Blake B, Zylka MJ. Prostatic acid phosphatase is expressed in peptidergic and nonpeptidergic nociceptive neurons of mice and rats. *PLoS One* 2010;5:e8674.
- [41] Wu CH, Ho WY, Lee YC, Lin CL, Hsieh YL. EXPRESS: NGF-trkA signaling modulates the analgesic effects of prostatic acid phosphatase in resiniferatoxin-induced neuropathy. *Mol Pain* 2016;12:1–8.
- [42] Wu WP, Hao JX, Halldner L, Lovdahl C, DeLander GE, Wiesenfeld-Hallin Z, Fredholm BB, Xu XJ. Increased nociceptive response in mice lacking the adenosine A1 receptor. *PAIN* 2005;113:395–404.
- [43] Yegutkin GG. Nucleotide- and nucleoside-converting ectoenzymes: important modulators of purinergic signalling cascade. *Biochim Biophys Acta* 2008;1783:673–94.
- [44] Zimmermann M. Ethical guidelines for investigations of experimental pain in conscious animals. *PAIN* 1983;16:109–10.
- [45] Zur Nedden S, Eason R, Doney AS, Frenguelli BG. An ion-pair reversed-phase HPLC method for determination of fresh tissue adenine nucleotides avoiding freeze-thaw degradation of ATP. *Anal Biochem* 2009;388:108–14.
- [46] Zylka MJ. Pain-relieving prospects for adenosine receptors and ectonucleotidases. *Trends Mol Med* 2011;17:188–96.
- [47] Zylka MJ, Sowa NA, Taylor-Blake B, Twomey MA, Herrala A, Voikar V, Vihko P. Prostatic acid phosphatase is an ectonucleotidase and suppresses pain by generating adenosine. *Neuron* 2008;60:111–22.